Mol. Cryst. Liq. Cryst., Vol. 530: pp. 83/[239]–90/[246], 2010

ISSN: 1542-1406 print/1563-5287 online
DOI: 10.1080/15421406.2010.495912

Taylor & Francis
Taylor & Francis Group

Highly Efficient Phosphorescent Green Organic Light-Emitting Diodes with High Energy Gap Host Materials

HOE MIN KIM,[1] JI HYUN SEO,[1] KUM HEE LEE,[2] HYUN JU KANG,[2] SEUNG SOO YOON,[2] AND YOUNG KWAN KIM[1]

[1]Department of Information Display, Hongik University, Seoul, Korea
[2]Department of Chemistry, Sungkyunkwan University, Suwon, Korea

We investigated the electroluminescent characteristics of three devices which were fabricated with a green phosphorescent emitter bis[2-(o-terphen-3-yl)pyridinato-C,N] iridium(III) (acetylacetonate) [$(tppy)_2Ir(acac)$] doped in triphenylsilane-based host materials, such as 4,4′-bis(triphenylsilyl)biphenyl (BSB), 9,9′-spirobifluorene-2-yltriphenylsilane (SFS) and (4-(10-(naphthalene-2-yl)anthracen-9-yl)phenyl)-triphenylsilane (ANPTPS), which have the different the triplet energy levels (E_T) of 2.61 eV, 2.64 eV and <1.91 eV, respectively. Among those, two devices using BSB and SFS hosts with the suitable E_T energy levels to green phosphorescent dopant exhibited the highly efficient green electrophosphorescence with the maximum luminous efficiencies of 51.3 cd/A and 46.6 cd/A, respectively, and the maximum quantum efficiencies of 13.9% and 12.4%, respectively.

Keywords Green phosphorescent host; organic light-emitting diode; triphenylsilane; triplet energy level

Introduction

Since the discovery of organic light-emitting diodes (OLEDs) by Tang and VanSlyke, there have been many studies to enhance the quantum efficiency of OLEDs. In order to obtain high efficiency of OLEDs, the phosphorescent OLEDs based on transition metal complexes such as iridium complexes have been studied, which emit phosphorescence from their triplet states, realizing nearly 100% internal quantum efficiencies of electroluminescence [1–5]. For efficient phosphorescent OLEDs, the development of suitable host materials is needed because the heavy-metal materials are normally doped into host materials. Up to now, the host materials for green electrophosphorescence are mainly based on arylamine derivatives, such as triphenylamine-triphenylsilane hybrids (BTPASi) [6], fluorene-triphenylamine

Address correspondence to Prof. Seung Soo Yoon, Department of Chemistry, Sungkyunkwan University, 300 Cheoncheon-dong, Jangan-gu, Suwon, Gyeonggi-do 440-746, Korea (ROK). Tel.: (+82)31-290-7071; Fax: (+82)31-290-7075; E-mail: ssyoon@skku.edu

hybrids (TFTPA) [7] and carbazole-fluorene hybrid (DFC) [8], and carbazole oligomer [9] as well as common phosphorescent host materials such as CBP and mCP. However, the electroluminescent properties of green phosphorescent host materials require further improvement for application in full-colored flat panel displays. A prerequisite of the suitable hosts for the efficient green phosphorescent OLEDs is that the triplet excited state (E_T) of hosts materials should be higher than that of the phosphorescent dopants [10], since the excitons formed from the phosphorescent emitting dopant has to be confined within its excited energy state to achieve high quantum efficiency in phosphorescent OLEDs by preventing reverse energy transfer from the dopant back to the host [11–14].

In this paper, we described three green phosphorescent OLEDs using bis[2-(o-terphen-3-yl)pyridinato-C,N]iridium(III) (acetylacetonate) [$(tppy)_2Ir(acac)$] as a dopant, and triphenylsilane-based host materials, such as (4-(10-(Naphthalene-2-yl)anthracen-9-yl)phenyl)triphenylsilane (ANPTPS), 4,4′-Bis(triphenylsilyl)biphenyl (BSB) and 9,9′-(Spirobifluorene-2-yl)triphenylsilane (SFS), to explore the effect of new three host materials with the different E_T on the EL efficiencies of OLEDs using them. As will be demonstrated below, the variations of E_T in host materials lead to significant difference in the device performances of the green phosphorescent OLED devices.

Device Fabrication

We fabricated three green phosphorescent OLEDs with a structure of indium tin oxide (ITO) (150 nm, anode)/4,4′-bis[N-(naphthyl)-N-phenyl-amino]biphenyl (NPB) (50 nm, hole transporting layer)/Host doped with 8% bis[2-(o-terphen-3-yl)pyridinato-C,N]iridium(III) (acetylacetonate) [$(tppy)_2Ir(acac)$] (30 nm, emission layer)/4,7-diphenyl-1,10-phenanthroline (BPhen) (30 nm, hole blocking and electron transporting layer)/lithium quinolate (Liq) (2 nm, electron injection layer)/aluminum (Al) (100 nm, cathode), where ANPTPS, BSB and SFS were used as host materials. $(tppy)_2Ir(acac)$ was used as green-emitting dopant. The chemical structures of host and dopant materials used in this study were shown in the Figure 1. The ITO on

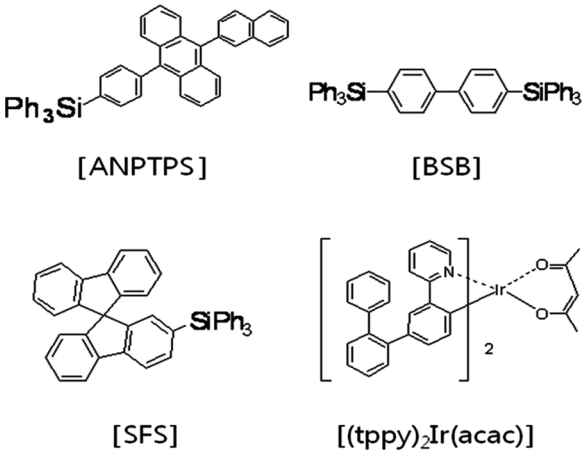

Figure 1. Chemical structures of host and dopant materials used in this study.

glass substrates with a sheet resistance of 30 Ω/sq (emitting region was $3 \times 3\,mm^2$) was used as a transparent anode. The ITO glass was chemically cleaned in an ultrasonic bath by following sequence: acetone, methanol, de-ionized water and isopropyl alcohol. After the cleaned ITO substrates had been dried by using N_2 gas. Then, pre-cleaned ITO was treated by Oxygen plasma with the power conditions of 125 W for 2 min. under low vacuum of 2×10^{-2} torr. All organic layers were deposited in succession by high vacuum (5×10^{-7} torr) thermal evaporation at a rate of 1.0 Å/sec and 0.1 Å/sec for Liq, respectively. After, the deposition of the organic layers without a vacuum break, the Al cathode was vacuum deposited to a thickness of 100 nm at a rate of 10 Å/sec.

Materials

ANPTPS [15], BSB [16], and $(tppy)_2Ir(acac)$ [17] were prepared according to published methods. On the other hand, SFS is novel host material developed from our laboratory. SFS was synthesized by following method; A solution of 2-Bromospirofluorene (0.9 g, 2.48 mmol) in THF (20 mL) was stirred at −78°C under N_2 for 10 min. A solution of *n*-Butyllithium (2.3 mL, 3.72 mmol 1.6 M in hexane) was slowly added and the solution stirred for 1 h. A solution of chlorotriphenylsilane (0.8 g, 2.98 mmol) in THF(10 mL) was added, and the resulting mixture was warmed slowly to room temperature and then stirred for 2 h. When the reaction was complete, water was added to quench. The product was extracted with Ethyl acetate and washed with brine and H_2O and the organic layer dried over anhydrous $MgSO_4$ and the solvent removed in vacuo. As a result, SFS was obtained as a white solid (0.82 g, 59%) after recrystallization from CH_2Cl_2/hexane. ^{1}H-NMR (300 MHz, $CDCl_3$. ppm 7.85–7.74 (m, 4H), 7.48 (d, $J = 8.5$ Hz, 1H), 7.39–7.29 (m, 13H), 7.25–7.20 (m, 5H), 7.13–7.06 (m, 4H), 6.77–6.71 (m, 3H): ^{13}C-NMR (125 MHz, $CDCl_3$. ppm 148.9, 148.5, 142.0, 136.5, 136.4, 134.4, 132.3, 129.7, 128.5, 128.0, 127.9, 127.8, 124.4, 124.1, 120.5, 120.3, 119.9: MS(EI^+) m/z 574 (M^+). Anal. calcd for $C_{43}H_{30}Si$: C 89.85, H 5.26 found: C 89.78, H 5.31.

Measurements

The current density–voltage (J-V) characteristics of the OLEDs were measured with a source measure unit (Keithley 236) with the DC voltage bias, the optical and electrical properties of the devices such as the luminance, luminous efficiency, Commission International de L'Eclairage (CIE) coordinates and electroluminescence (EL) spectra characteristics were analyzed by CHROMA METER CS-1000 instruments. All measurements were carried out under ambient conditions at room temperature. The energy band gaps were determined by UV spectrum PL method and the energy levels were measured with a low-energy photo-electron spectrometer (Riken-Keiki, AC-2). Moreover, the E_T energy levels were measured with a low temperature PL spectrometer.

Results and Discussion

Figure 2 shows the current density flow versus voltage of devices using three host materials. The current densities of devices using ANPTPS, BSB and SFS hosts are 9.20 mA/cm^2, 0.43 mA/cm^2, and 0.13 mA/cm^2 at applied voltage of 8 V, respectively. Interestingly, the device using ANPTPS host shows the much superior current

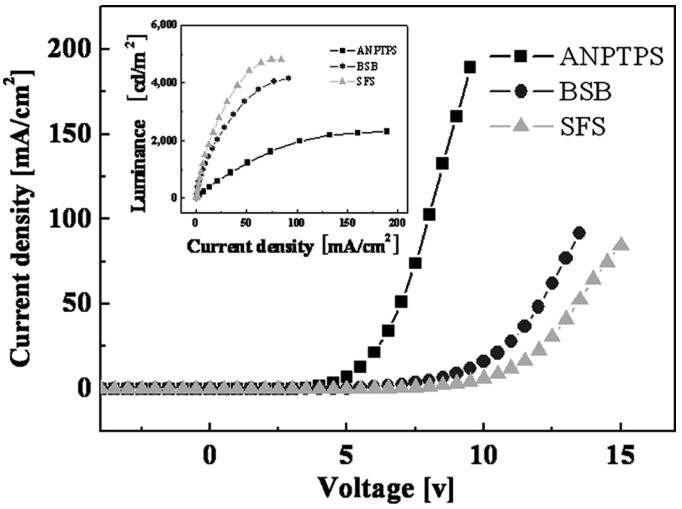

Figure 2. Current density versus voltage (inset; luminance versus current density) curves of devices using various host materials, respectively.

density flow than those using BSB and SFS hosts. As shown in the energy level diagram of Figure 3, the HOMOs of ANPTPS, BSB, and SFS have energy barrier of 0.3 eV, 1.0 eV, and 0.7 eV, respectively, with HOMO of NPB. Also, the LUMOs of ANPTPS, BSB, and SFS have energy barrier of 0.3 eV, 0.7 eV, and 0.8 eV, respectively, with LUMO of Bphen. These observations indicate that, among three devices using three different hosts, a device using ANPTPS host has the lowest injection barrier for both hole and electron, and thus the charge injection of the device using ANPTPS host is the easiest. Presumably, these differences in charge injection barriers would contribute to the differences in the current density flow of devices. However, the possibility of the contribution of the other factor such as charge mobility in the emitting layers to the current density flow of devices could not be excluded.

Also, the luminance versus the current density flow of devices using three host materials is shown in Figure 2. The devices using BSB, SFS, and ANPTPS hosts show the luminance of 1432 cd/m^2, 2300 cd/m^2, and 924 cd/m^2, respectively, at

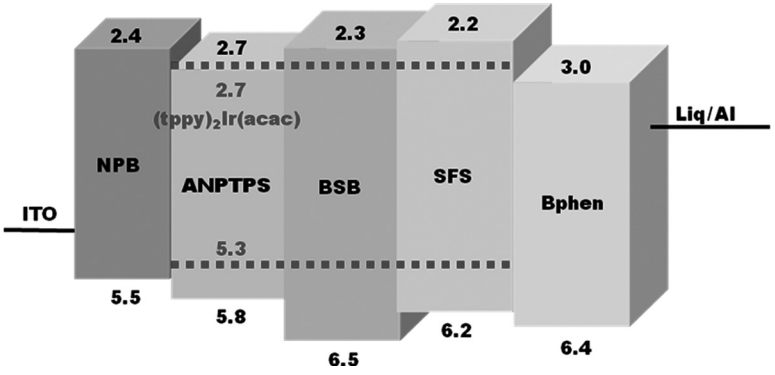

Figure 3. Energy band levels of materials used in this study.

Table 1. Optical properties of compounds used in this study

	λ_{Abs}[a] [nm]	λ_{em}[a] [nm] at RT	λ_{em}[b] [nm] at 77 K	HOMO/ LUMO[c] [eV]	E_g	Φ[d]
ANPTPS	377	422	>650[e] (<1.91 eV)	5.77/2.72	3.05	0.86
BSB	272	323	475 (2.61 eV)	6.49/2.33	4.16	0.83
SFS	229	320	470 (2.64 eV)	6.16/2.20	3.96	0.09
$(tppy)_2$ Ir(acac)	414(0.40), 468(0.35)	526	556 (2.23 eV)	5.25/2.68	2.57	0.32

[a]Maximum absorption or emission wavelength, measured in CH_2Cl_2 solution.
[b]Phosphorescent emission in 2-methyl-THF solution at 77 K. The triplet energy (E_T) calculated is included in the parenthesis.
[c]Obtained from AC-2 and UV-vis absorption measurements.
[d]Using DPA as a standard; $\lambda_{ex} = 360$ nm ($\lambda = 0.90$ in CH_2Cl_2).
[e]not observed up to 650 nm.

applied voltage of 9.5 V. We expected that T1 energy level of host materials in devices has influence on the light emission of device. In the device using ANPTPS host, E_T of ANPTPS was estimated less than 1.91 eV by the measurement of phosphorescent emission in 2-methyl-THF solution at 77 K, as shown in Table 2. This E_T value of ANPTPS host is less than that of green phosphorescent dopant $(tppy)_2$ Ir(acac) ($E_T = 2.23$ eV) used in this study. This imply that the excitons formed on the phosphorescent emitting dopant could not be confined within its excited energy state due to the reverse energy transfer from the dopant back to the host, and thus lead to the low EL efficiencies of device using ANPTPS host. In the devices using BSB and SFS hosts, the BSB and SFS have adequate high E_T energy level ($2.61 \sim 2.63$ eV) compared with green phosphorescent dopant $(tppy)_2$Ir(acac) ($E_T = 2.23$ eV), as shown in Table 2. Thus, excitons are confined within its excited energy state of dopant in the devices using BSB and SFS hosts, and leads to the improved EL efficiencies of devices. However, in the devices using BSB and SFS hosts, the formation of excitons on dopant materials by energy transfer between host and dopant seems to be ineffective because the injection barriers of hole and electron

Table 2. Optical and electrical characteristics of devices in this study

Host materials	J[a] [mA/cm^2]	L[b] [cd/m^2]	LE[c/d] [cd/A]	PE[c/d] [lm/W]	QE[c/d] [%]	CIE[e]	λ_{em}[f] [nm]
ANPTPS	9.20	924	4.8/2.9	5.0/1.5	1.3/0.8	(0.34, 0.55)	530
BSB	0.43	1432	51.3/9.8	53.1/2.9	13.9/2.67	(0.35, 0.61)	529
SFS	0.13	2300	46.6/12.9	36.5/3.40	12.4/3.60	(0.35, 0.56)	527

[a]Maximum current density. At 8.0 V.
[b]Maximum luminance. At 9.5 V.
[c]Maximum value.
[d]At 20 mA/cm^2.
[e]CIE coordinate (x, y) at 8.0 V.
[f]Maximum emission wavelength of devices at 8.0 V.

into BSB and SFS are high, relative to device using ANPTPS host. The direct carrier trapping mechanism seems to be effective in the devices using BSB and SFS hosts. Particularly, the direct hole trapping from NPB to dopant $(tppy)_2Ir(acac)$ near NPB interface in the emitting layer seems to be main mechanism for the formation of excitons. In this situation, the electron injection barrier and mobility of host materials is a crucial factor in the efficient EL emission because electron should be reached to NPB interface in the emitting layer to form excitons. Presumably, the small differences in EL efficiencies between the devices using BSB and SFS hosts might be originated from the differences in the electron injection barrier and mobility of host materials such as BSB and SFS. The luminance efficiency, power efficiency, and quantum efficiency versus current density of devices are shown in Figure 4, the inset of Figures 4 and 5, respectively. And the results are summarized in Table 1. The maximum luminous efficiencies of devices using ANPTPS, BSB, and SFS hosts are 4.8 cd/A, 51.3 cd/A, and 46.6 cd/A, respectively. The maximum power efficiencies of devices using ANPTPS, BSB, and SFS hosts are 5.0 lm/W, 53.1 lm/W, and 36.5 lm/W, respectively. Moreover, these devices have maximum quantum efficiencies of 1.3%, 13.9%, and 12.4%, respectively. As a result, we could confirm that the high E_T of host materials leads to the improved device efficiency. However, the possibility of the contribution of the other factors such as charge balance in the emitting layers and the extent of carrier trapping by dopant materials to the EL efficiencies of devices could not be excluded.

Figure 6 and the inset of Figure 6 show the electroluminescence (EL) spectra and CIE coordinates of devices using various host materials, respectively. EL spectra were obtained when the voltage of 8 V was applied. They show the strong main emission peak at near about 527 nm due to green emitting dopant, $(tppy)_2Ir(acac)$ with the CIE coordinates of $(0.34 \pm 0.01,\ 0.58 \pm 0.03)$. Interestingly, devices using ANPTPS and BSB hosts have weak emission peak at near about 440 nm which is assigned to NPB emissions due to the exciton leakage from the emitting layer into NPB layer. Presumably, these exciton leakage might take place due to the smaller

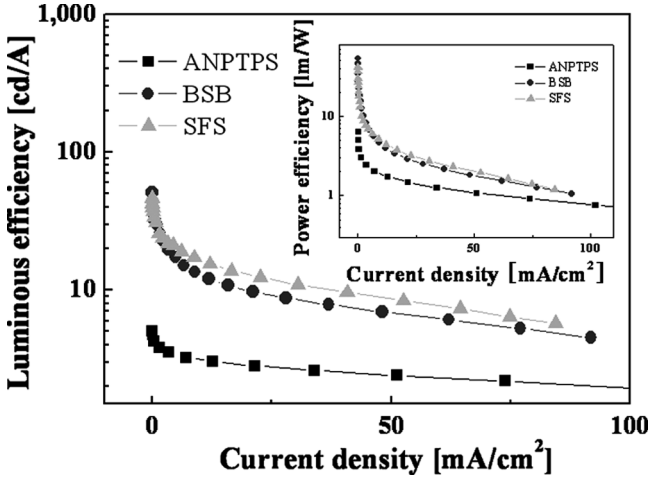

Figure 4. Luminous efficiency (inset; power efficiency) versus current density curves of the devices using various host materials.

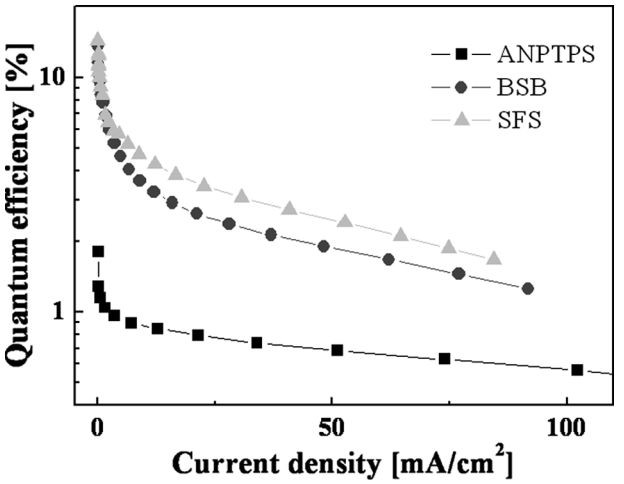

Figure 5. Quantum efficiency versus current density curves of the devices using various host materials.

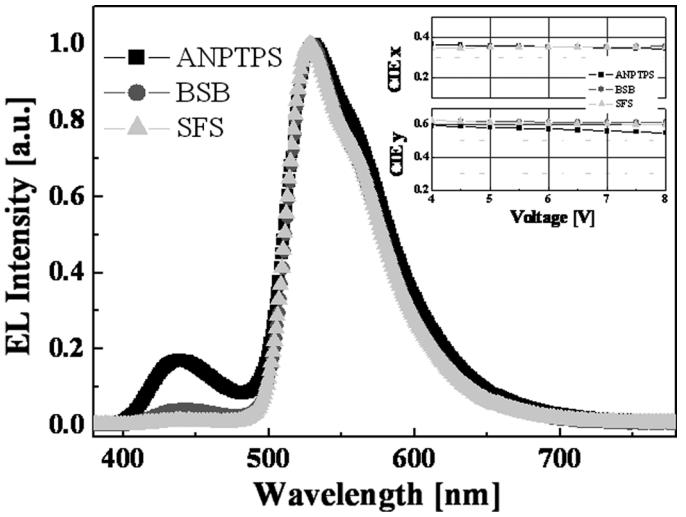

Figure 6. EL spectra (inset; CIE_{xy} coordinates) of the devices using various host materials.

E_T of host than that of dopant for device using ANPTPS host, and the mismatch of charge mobility of host materials for device using BSB host. Intriguingly, this study suggests that SFS is a candidate for the future development of host materials for green phosphorescent OLEDs with the improved EL performances, because it has the suitable E_T value and the well-matched charge mobility, as shown above.

Conclusions

We have successfully developed two host materials such as BSB and SFS with the suitable triplet energy level (E_T) for green phosphorescent OLEDs. By using them

as hosts with bis[2-(o-terphen-3-yl)pyridinato-C,N]iridium(III) (acetylacetonate) as a dopant, two highly efficient green electrophosphorescent OLED were successfully fabricated with the maximum luminous efficiencies of 51.3 cd/A and 46.6 cd/A, respectively, and the maximum quantum efficiencies of 13.9% and 12.4%, respectively. This study indicate that the suitable E_T energy level of host material as well as the other factor such as charge balances in the emitting layer are crucial factors for the efficient EL performances in green electrophosphorescent OLEDs.

Acknowledgments

This work was supported by Energy Resources Technology Development program (2007-E-CM11-P-07) and Strategy Technology Development program (10030834) from Ministry of Knowledge Economy (MKE).

References

[1] Tang, C. W., & VanSlyke, S. A. (1987). *Appl. Phys. Lett.*, *51*, 913.
[2] Baldo, M. A., Lamansky, S., Burrows, P. E., Thompson, M. E., & Forrest, S. R. (1999). *Appl. Phys. Lett.*, *75*, 4.
[3] Baldo, M. A., O'Brien, D. F., You, Y., Shoustikov, A., Thompson, M. E., & Forrest, S. R. (1998). *Nature*, *395*, 151.
[4] Kelly, S. M. (2000). *Flat Panel Display: Advanced Organic Materials*, Royal Society of Chemistry: London.
[5] Holmes, R. J., Forrest, S. R., Tung, Y. J., Kwong, R. C., Brown, J. J., Garon, S., & Thompson, M. E. (2003). *Appl. Phys. Lett.*, *82*, 2422.
[6] Jiang, Z., Chen, Y., Fan, C., Yang, C., Wang, Q., Tao, Y., Zhang, Z., Qin, J., & Ma, D. (2009). *Chem. Comm.*, 3398.
[7] Shih, P.-I., Chien, C.-H., Wu, F.-I., & Shu, C.-F. (2007). *Adv. Funct. Mater.*, *17*, 1.
[8] Wong, K.-T., Chen, Y.-M., Lin, Y.-T., Su, H.-C., & Wu, C.-C. (2005). *Org. Lett.*, *7*, 5361.
[9] Brunner, K., van Dijken, A., Borner, H., Bastiaansen, J., Kiggen, N., & Langeveld, B. (2004). *J. Am. Chem. Soc.*, *126*, 6035.
[10] Su, S.-J., Sasabe, H., Takeda, T., & Kido, J. (2008). *Chem. Mater.*, *20*, 1691.
[11] O'Brien, D. F., Baldo, M. A., Forrest, S. R., & Thompson, M. E. (1999). *Appl. Phys. Lett.*, *74*, 442.
[12] Adachi, C., Kwong, R. C., Djurovich, P., Adamovich, V., Baldo, M. A., Thompson, M. E., & Forrest, S. T. (2001). *Appl. Phys. Lett.*, *79*, 2082.
[13] Baldo, M. A., Thompson, M. E., & Forrest, S. R. (1999). *Pure Appl. Chem.*, *71*, 2095.
[14] Kim, S. H., Jang, J., & Lee, J. Y. (2007). *Appl. Phys. Lett.*, *90*, 223505.
[15] Ito, M. Preparation of arylsilanes and organic electroluminescent device utilizing the same. WO 200712970, 20071125.
[16] Lin, J.-J., Liao, W.-S., Huang, H,-J., Wu, F.-I., & Cheng, C.-H. (2008). *Adv. Funct. Mater.*, *18*, 485.
[17] Lee, K. H., Seo, J. H., Kim, Y. K., & Yoon, S. S. (2009). *J. Nanosci., Nanotechno.*, *9*, 7099.